ISSN 0023-1584, Kinetics and Catalysis, 2015, Vol. 56, No. 6, pp. 781–787. © Pleiades Publishing, Ltd., 2015.
Original Russian Text © L.A. Isupova, N.A. Kulikovskaya, N.F. Saputina, E.Yu. Gerasimov, S.V. Tsybulya, 2015, published in Kinetika i Kataliz, 2015, Vol. 56, No. 6, pp. 770–776.

$La_{1-x}Ca_xFeO_{3-\delta}$ ($x = 0–1$) Perovskites Prepared by the Pechini Method: Catalytic Activity in Deep Methane and CO Oxidation

L. A. Isupova*, N. A. Kulikovskaya, N. F. Saputina, E. Yu. Gerasimov, and S. V. Tsybulya

Boreskov Institute of Catalysis, Siberian Branch, Russian Academy of Sciences, Novosibirsk, 630090 Russia

**e-mail: isupova@catalysis.ru*

Received January 22, 2015

Abstract—The catalytic activity of a series of $La_{1-x}Ca_xFeO_{3-\delta}$ ($x = 0–1$) materials prepared by the Pechini method from polymer–salt stocks has been investigated, and the phase composition and microstructure of these materials before and after testing them in methane oxidation have been determined. The activity and stability of the materials depends on their composition and on the reaction temperature. The introduction of calcium into lanthanum ferrite up to $x = 0.5$ causes a nonmonotonic increase in the activity of the catalyst in methane oxidation. As x is further increased, the catalytic activity falls off. It has been analyzed how the activity of the catalysts is affected by variations of their imperfection and microstructure as a result of the introduction of calcium and under the action of the reaction medium. According to high-resolution transmission electron microscopy data, under the action of the reaction medium the perovskite structure undergoes partial degradation (in subsurface layers) leading to the formation of planar defects and to the release of iron oxide nanoparticles.

Keywords: perovskites, $La_{1-x}Ca_xFeO_{3-\delta}$, microstructure, methane and CO oxidation, stability

DOI: 10.1134/S0023158415050092

INTRODUCTION

The $La_{1-x}M_xFeO_{3-\delta}$ (M = Ca, Sr, Ba) perovskites are promising materials for a number of high-temperature processes. They are usable in high-temperature electrochemical devices, gas sensors, oxygen-permeable membranes, etc. [1–3]. $La_{1-x}M_xFeO_{3-\delta}$ solid solutions approved themselves as catalysts for various reactions, including deep methane oxidation in the presence and absence of oxygen in the gas phase, oxidative methane condensation, ammonia oxidation, and nitrous oxide decomposition [4–7].

The physicochemical properties of substituted perovskites are known to depend on the conditions under which they were prepared. For example, homogeneous solid solutions form in the $La_{1-x}Ca_xFeO_{3-\delta}$ ($x = 0–0.5$) system prepared from citrates by calcination in air at 800°C [7]. By contrast, no homogeneous solid solutions were detected in the systems obtained by a ceramic synthesis using calcination at 1400°C. A homological series of three phases, namely, $LaFeO_3$ (perovskite structure), $LaCa_2Fe_3O_8$ (vacancy-ordered perovskite-like phase with a Grenier structure), and $Ca_2Fe_2O_5$ (vacancy-ordered perovskite-like phase with a brownmillerite structure) forms in this case, and these phases form no solid solution [8]. Our earlier studies [9–11] demonstrated that the ceramic $La_{1-x}Ca_xFeO_{3-\delta}$ samples prepared by calcination in air at 1100°C consist of a homogeneous solid solution up to $x = 0.2$ and the samples obtained by the mechanochemical method with calcination in air at 900°C for 4 h are homogeneous solid solutions up to $x = 0.4$. A wider composition range for the formation of $La_{1-x}Ca_xFeO_{3-\delta}$ solid solutions ($x = 0–0.7$) was observed for the samples prepared by the Pechini method and calcined at 800°C for 4 h [12]. It was demonstrated by high-temperature in situ X-ray diffraction that, as the $x = 0.7$ sample is heated in air or in a vacuum (residual pressure of $\sim 10^{-2}$ Torr), it remains stable up to 800°C. However, as the $x = 0.5–0.7$ samples are heated in air or in a vacuum to 1000°C, their X-ray diffraction patterns, showing diffraction peaks characteristic of the perovskite structure, begin to display reflections from a Grenier vacancy-ordered phase and a diffuse scattering peak that is presumably due to the microheterogeneous 1D nanostructure that was earlier detected by us in ceramic samples [12]. It was also demonstrated that the $x = 0–0.4$ samples undergo polymorphic transitions accompanied by oxygen evolution as they are heated and the transition temperature decreases with an increasing x [13, 14].

The marked dependence of the phase composition and microstructure of the perovskites on their synthesis conditions is a possible cause of controversy in the literature concerning the perovskites' catalytic activity. Tests of $x = 0–1$ samples prepared by ceramic synthe-

sis (1100°C) and by the mechanochemical method (900 and 1100°C) [9–11] revealed a maximum at $x = 0.3–0.6$ in their specific catalytic activity in the oxidation of CO (300–500°C; reaction mixture: 1% CO + 1% O_2, He balance) and methane (350–600°C; reaction mixture: 0.5% CH_4 + 9% O_2, He balance). In the authors' opinion, the activity maximum arises from the microheterogeneity of these two-phase samples, which are characterized by a high phase boundary density in the middle-composition region and, accordingly, by a large proportion of weakly bonded oxygen surface species as a consequence of oxygen insertion into phase boundaries [15]. It was demonstrated [7] that, in the methane oxidation reaction (reaction mixture: 0.4% CH_4 + 10% O_2, He balance), the methane conversion at 350–600°C is practically independent of the composition of the solid solution ($x = 0–0.4$) and the lower conversion observed with the $x = 0.5$ sample is explained by its smaller specific surface area. Conversely, for the homogeneous $x = 0–0.4$ samples synthesized from citrates (700°C) there is a correlation between their activity (in terms of 50% conversion temperature) in methane oxidation (reaction mixture: 0.37% CH_4 + 23.22% O_2, He balance) and the degree of substitution, which leads to an increase in the proportion of Fe^{+4} cations in the oxide or to an increase in the amount of the weakly bonded oxygen species that results from the substitution. It is also possible that the difference in catalytic activity between the samples prepared by different methods is due not only to the difference between their initial compositions but also to changes in the degree of imperfection and structure of the oxide under the action of reaction media that are poorer in oxygen than air. It was demonstrated [17] that the residual oxygen content of the oxide (or δ) depends on the temperature and atmosphere composition and, according to earlier data [13, 14], this dependence can lead to various changes in the $La_{1-x}Ca_xFeO_{3-\delta}$ structure (ranging from the appearance of vacancies to the formation of vacancy-ordered phases).

The purpose of this study was to determine the catalytic activity of $La_{1-x}Ca_xFeO_{3-\delta}$ homogeneous solid solutions synthesized by the Pechini method in methane and CO oxidation and to investigate the effect of the reaction medium on the structural properties of the oxides.

EXPERIMENTAL

$La_{1-x}Ca_xFeO_{3-\delta}$ samples with the degree of substitution varied in $x = 0.1$ steps were synthesized by the polymerizable precursor (Pechini) method. For this purpose, appropriate amounts of aqueous solutions of lanthanum, calcium, and iron nitrates were combined, citric acid and ethylene glycol were added, and the mixture was evaporated at 70–80°C until the formation of a resinous polymer (polymer–salt stock). The polymer was subjected to oxidative destruction, and the product was calcined at 800°C.

X-ray diffraction patterns of samples were recorded using an X'TRA diffractometer (Switzerland) with CuK_α radiation ($2\theta = 0.02°$ scanning steps; counting time of 5 s per data point).

High-resolution electron micrographs were obtained on a JEM 2010 microcope (Japan) with a resolution of up to 1.4 Å. Energy-dispersive X-ray (EDX) microanalyses of oxides for determining their elemental composition were carried out using an EDX spectrometer with a Si(Li) detector at an energy resolution of 130 eV.

The catalytic activity of oxides in methane oxidation was measured using a flow-through setup at 350–600°C. A catalyst (1 g, 0.25–0.5 mm fraction) was mixed with quartz (1 cm^3) and was placed in a U-shaped quartz reactor with an inner diameter of 4.5 mm. The flow rate of the feed (0.9% CH_4 + 9% O_2, N_2 balance) was 2.4 L/h. Before taking measurements, the sample was kept in the reaction mixture for ~30 min at the preset temperature. After catalytic tests performed at 600°C, the sample was cooled to 450°C in the reaction mixture and its activity was measured again. The only methane oxidation products were carbon dioxide and water. The rate of the reaction was calculated using the following formula under the assumption that the process takes place in the plug flow regime:

$$w = 2.69 \times 10^{19} k C_0, \text{ (CH}_4\text{ molecules) m}^{-2}\text{ s}^{-1},$$

where k is the rate constant defined as $k = \ln(1 - X_{CH_4})/\tau S_{BET}\, m$, $m^{-2}\ s^{-1}$ (X_{CH_4} is the methane conversion, τ is the residence time (s), and S_{BET} is the specific surface area of the sample (m^2/g)) and C_0 is the initial methane concentration.

Catalytic activity in CO oxidation was determined using a flow circulation setup and a catalyst particle size fraction of 0.25–0.5 mm. A catalyst (1 g), mixed with quartz (1 cm^3), was placed in a tubular quartz reactor 15 mm in diameter. The flow rate of the feed (1% CO + 1% O_2, N_2 balance) was 10 L/h, and the circulation rate was 1000 L/h. Prior to performing catalytic tests, the sample was kept in flowing artificial air (20% O_2 + 80% N_2, 5 L/h) at 400°C for 1 h and was then cooled. Before each measurement, the sample was kept in the reaction mixture at the preset temperature for 30 min. The rate of the reaction was determined using the following formula under the assumption that the process takes place in the perfect-mixing regime:

$$w = 7.47 \times 10^{17} X_{CO}/(1 - X_{CO}), \text{ (CO molecules) m}^{-2}\text{s}^{-1},$$

where X_{CO} is the CO conversion.

After the tests carried out at 300, 350, 400, 450, and 500°C, the sample was cooled to 350°C in the flowing reaction mixture and its activity was measured again.

Specific surface areas were measured by the BET method using thermal argon desorption.

Methane conversion over $La_{1-x}Ca_xFeO_{3-\delta}$ samples at 350–600°C and the specific surface areas of the samples before and after catalytic tests

Entry	Composition	S_{BET}, m^2/g		Methane conversion, %, at different temperatures, °C						
		before testing	after testing	350	400	**450**	500	550	600	**450***
1	$LaFeO_{3-\delta}$	9.4	11	10.9	36.8	**72.4**	97.3	99.6	100	**72.4**
2	$La_{0.9}Ca_{0.1}FeO_{3-\delta}$	7.2	10	12.2	43.6	**84.8**	100	100	100	99.6**
3	$La_{0.8}Ca_{0.2}FeO_{3-\delta}$	9.4	12	15.7	50.1	**89.9**	100	100	–	**86.6**
4	$La_{0.7}Ca_{0.3}FeO_{3-\delta}$	8.6	11	15.2	48.1	**86.6**	100	100	–	**83.9**
5	$La_{0.6}Ca_{0.4}FeO_{3-\delta}$	7.6	11	15.8	40.8	**84.4**	99.6	100		**75.3**
6	$La_{0.5}Ca_{0.5}FeO_{3-\delta}$	8.3	12	12.5	41.7	**82.2**	99.6	100	–	**76.1**
7	$La_{0.4}Ca_{0.6}FeO_{3-\delta}$	8.1	10	12.4	18.8	**71.5**	97.7	100	–	**69.8**
8	$La_{0.3}Ca_{0.7}FeO_{3-\delta}$	8.0	11	5.5	35.2	**69.6**	98.9	100	–	**70.1**
9	$La_{0.2}Ca_{0.8}FeO_{3-\delta}$	5.8	10	6.8	33.5	**70.3**	98.5	100	–	**68.9**
10	$La_{0.1}Ca_{0.9}FeO_{3-\delta}$	9.0	8.7	6.3	30.3	**63.9**	93.9	100	–	**57.1**
11	$CaFeO_{3-\delta}$	8.4	7.3	5.3	20.3	**49.2**	88.0	99.2	100	**38.2**

The boldfaced numbers are data obtained before and after testing at the same temperature.

* The test was performed after lowering the temperature from 600 to 450°C.

** 500°C.

RESULTS AND DISCUSSION

The table lists methane conversion data obtained at different testing temperatures for the $La_{1-x}Ca_xFeO_{3-\delta}$ (x = 0–1) catalysts prepared by the Pechini method. Even at 500°C, 100% methane conversion is achieved with all catalysts but the x = 0.9 and 1 samples. Note also that raising the calcium content from zero to x = 0.5 increases the methane conversion over the conversion observed for unsubstituted lanthanum ferrite at low testing temperatures; however, the methane conversion for $x > 0.5$ is lower than for $LaFeO_3$. In addition, for the $0.2 < x < 0.6$ and x = 0.8–1 samples we observed a decrease in methane conversion during the test. The methane conversion at 450°C at the beginning of the test is higher than the conversion at the end of the test, after 100% conversion at 600°C was reached and the temperature was lowered to 450°C. An increase in specific surface area is observed after testing for all catalysts except the x = 0.9 and 1 samples (table).

Figure 1 shows how specific catalytic activity (SCA) depends on the catalyst composition. SCA values were determined both as catalytic activity normalized to the specific surface area of the fresh samples and as catalytic activity normalized to that of the samples that had been tested (which had a stabilized surface area), and these two characteristics were found to vary with catalyst composition in essentially similar ways. Generally, the stabilized surface showed a lower SCA, indicating that the chemical composition of the oxide surface changes during the tests.

At low temperatures (350°C), the activity of the catalysts as a function of their composition changes only slightly. At a higher temperature of 400°C, the x = 0.1–0.5 and 0.7–0.9 samples show approximately equal activities and the activity of the x = 0, 0.6, and 1 samples is lower. As the temperature is raised to 450°C and above, two activity maxima appear in the composition ranges x = 0.1–0.5 and x = 0.8. Elevating

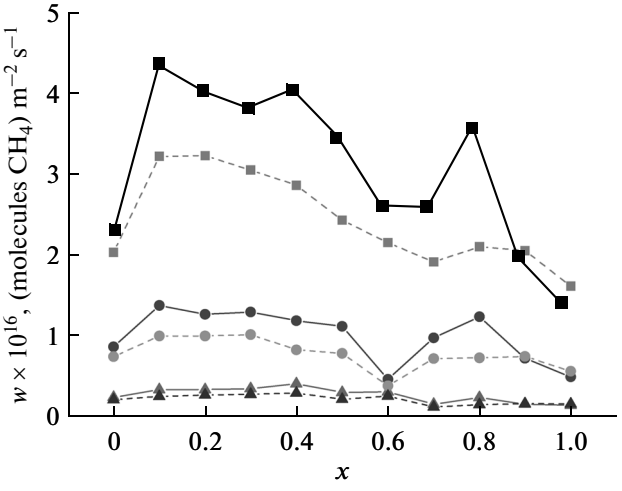

Fig. 1. Methane oxidation rate at (▲ 350, (●) 400, and (■) 450°C as a function of the oxide composition. Solid lines: reaction rate normalized to the specific surface area of the initial samples; dashed lines: reaction rate normalized to the specific surface area of the samples stabilized in the reaction medium.

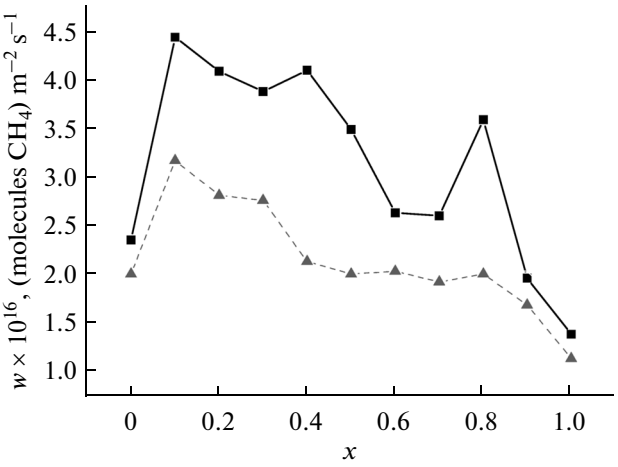

Fig. 2. Methane oxidation rate at 450°C as a function of the oxide composition under conditions of an (■) increasing and (▲) decreasing testing temperature. The calculations were carried out for the initial specific surface area (solid line) and for the specific surface area stabilized in the reaction medium.

the temperature increases the deference between the SCA values determined for the fresh and stabilized surfaces.

Figure 2 plots the dependence of SCA at 450°C on the oxide composition for the samples at the early stages of testing (with catalytic activity normalized to the specific surface area of fresh samples) and for the same samples that were tested at 600°C and were then cooled to 450°C (with catalytic activity normalized to the specific surface area of stabilized samples). These plots indicate that the SCA of some of the catalysts decreases in the course of testing. The samples that showed a lower initial activity (those with $x = 0$, 0.6, 0.9, and 1) turned out to be more resistant to the reaction medium. The increase in activity due to the introduction of calcium into lanthanum ferrite persists in the testing of the $x = 0.1$–0.3 samples as well, although to a lesser extent. The changes in SCA occurring under the action of the reaction medium, depending on the degree of substitution, may be due to restructuring occurring in the oxides as a consequence of the removal of part of the oxygen [12–14].

According to X-ray analysis data, the freshly prepared $La_{1-x}Ca_xFeO_{3-\delta}$ samples with $x = 0$–0.7 before catalytic tests are homogeneous solid solutions. At $x = 0.4$, there is a morphotropic transition, which is agreement with earlier data [12].

The catalytic tests in methane oxidation do not alter the phase composition of the oxides (Fig. 3), but only a small change in the unit cell volume is observed (Fig. 4). After the catalytic tests, the $x = 0$–0.4 samples are orthorhombic perovskites and the $0.5 \le x \le 0.7$ samples are cubic ones, as is indicated by their X-ray diffraction patterns showing no weak reflections characteristic of the orthorhombic perovskite phase. The $x = 0.8$ and 0.9 samples are mixtures of the cubic perovskite and brownmillerite phases. The $x = 1.0$ phase is brownmillerite $Ca_2Fe_2O_5$ containing traces of $CaFe_2O_4$.

Figures 5 and 6 present electron micrographs of two oxide samples examined before and after the catalytic tests. It was demonstrated by high-resolution electron microscopy that, in the fresh samples, which consist of micrometer-sized particles, at a calcium content of $x > 0.2$ there are planar defects in (101) planes and there are ~5-nm iron oxide particles on the surface. After the catalytic tests, the number of iron oxide nanoparticles on the sample surface is much larger than their number on the surface of the fresh

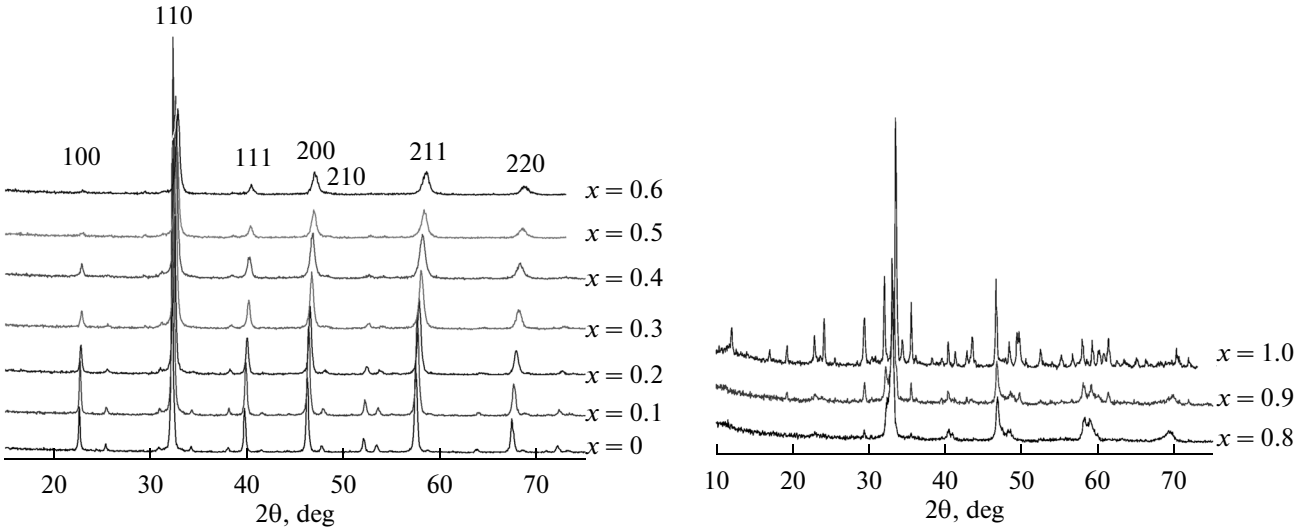

Fig. 3. X-ray diffraction patterns of $La_{1-x}Ca_xFeO_{3-\delta}$ samples recorded after catalytic tests.

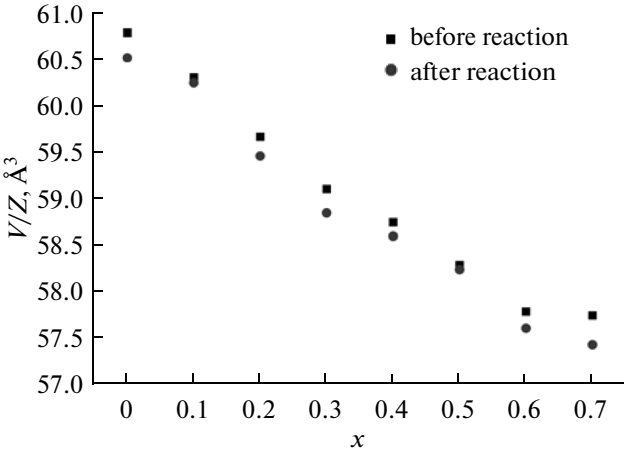

Fig. 4. Unit cell volumes of $La_{1-x}Ca_xFeO_{3-\delta}$ samples (■) before and (●) after carrying out the CH_4 oxidation reactions over them.

samples; at $x \geq 0.5$, these nanoparticles undergo segregation. Iron oxide nanoparticles are present in all of the samples that were subjected to catalytic testing, including the $x = 0$ sample. Near the planar defects, there is an overstoichiometric calcium concentration. Thus, the main difference between the fresh samples and the samples subjected to catalytic testing lies in the number and degree of segregation of planar defects in the bulk and in the concentration of nanosized iron oxide particles on the surface. The absence of iron oxide reflections in the X-ray diffraction patterns of all samples may be due the small size of the iron oxide particles (<5 nm) and their low concentration.

Our electron microscopic data significantly refined the results of X-ray diffraction analysis and demonstrated that the synthesized $La_{1-x}Ca_xFeO_{3-\delta}$ solid solutions are unstable in reaction media that contain less oxygen than atmospheric air does. They indicated the presence of iron oxide particles on the perovskite phase surface and the formation of planar defects in the bulk. The latter effect is likely due to the ordering of both cationic and anionic vacancies. Note, however, that these changes in microstructure evidently take place in relatively thin subsurface layers of the perovskite phase, since the X-ray diffraction patterns show no changes indicating the presence of planar defects in the bulk of the perovskite phase particles. It is not impossible that the increase in the specific surface area of the samples as a consequence of the catalytic tests is due to the release of the iron oxide nanoparticles.

Similar changes in the microstructure of particles under the action of the reaction medium or vacuum at 1100°C were observed by us in the $La_{1-x}Ca_xMnO_3$ system prepared by the Pechini method at $0.5 \leq x \leq 0.8$ [18, 19]. The formation of vacancy-ordered phases in calcium-substituted lanthanum ferrites with $x = 0.5$–0.7 upon at 1000°C even in the case of heat treatment in air [12–14] may be due to the ferrites being less stable than the manganites, in which these phases were not observed even upon severer heat treatment. It cannot be ruled out that the release of iron oxide nanoparticles and the formation of planar defects (which are possibly fragments of the layered perovskite structure) are the initial stage of the restructuring in the formation of vacancy-ordered phases with a Grenier or brownmillerite structure.

The data of this study suggest that the decrease in activity observed in the course of the catalytic tests arises from the formation of vacancy-ordered structures in the subsurface layers of the particles. This makes it clear why the unsubstituted ($x = 0$) samples

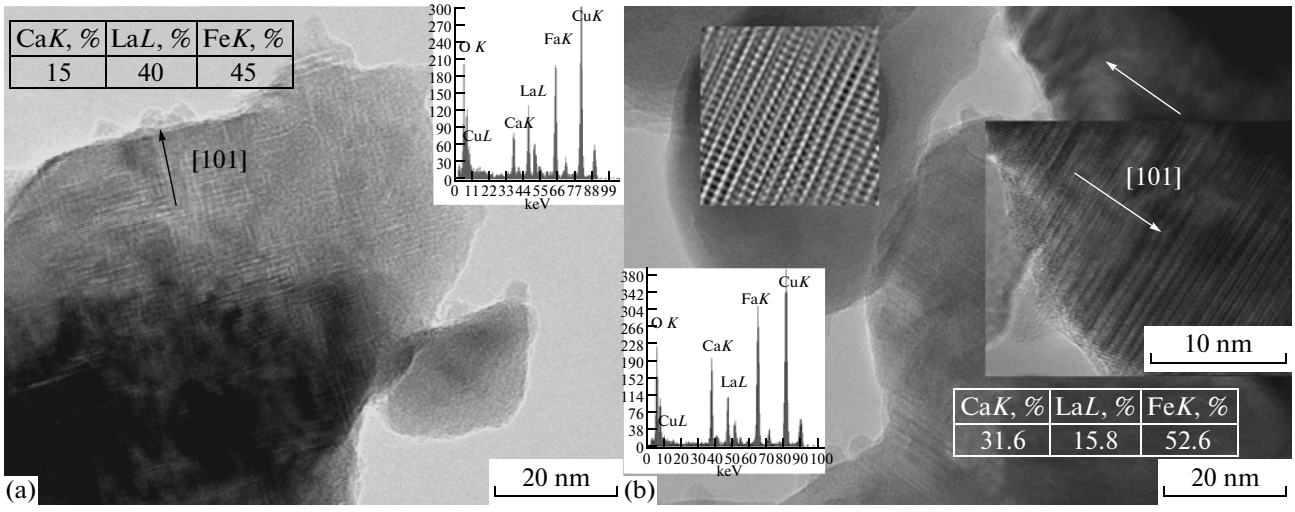

Fig. 5. Micrographs of (a) $La_{0.6}Ca_{0.4}FeO_{3-\delta}$ and (b) $La_{0.4}Ca_{0.6}FeO_{3-\delta}$ obtained before testing these samples in methane oxidation.

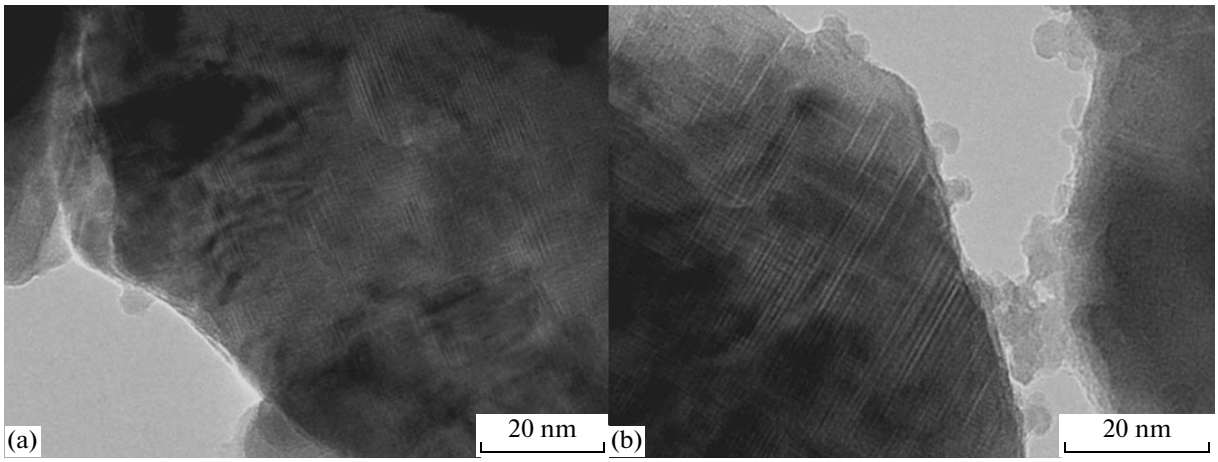

Fig. 6. Micrographs of (a) $La_{0.6}Ca_{0.4}FeO_{3-\delta}$ and (b) $La_{0.4}Ca_{0.6}FeO_{3-\delta}$ obtained after testing these samples in methane oxidation.

and samples with a high degree of substitution (x = 0.9–1) are more stable in the reaction medium: They either have only a small number of vacancies or contain vacancy-ordered phases. Apparently, an increase in the degree of substitution, which leads to the formation of a larger number of vacancies in the oxides as the temperature is raised, is favorable for the formation of vacancy-ordered structures. Indeed, the x = 0.4–0.5 samples are deactivated to a larger extent than the $x < 0.4$ samples (Fig. 2). This trend suggests that the lower yet more stable activity of the x = 0.6–0.7 samples, which have a high vacancy concentration, is solely due to the high rate of restructuring therein, which comes to completion before the reaction mixture is sampled for analysis in the catalytic tests. These data indicate that the vacancy ordering in the perovskites is markedly accelerated under the action of the methane-containing reaction medium, taking place below 600°C.

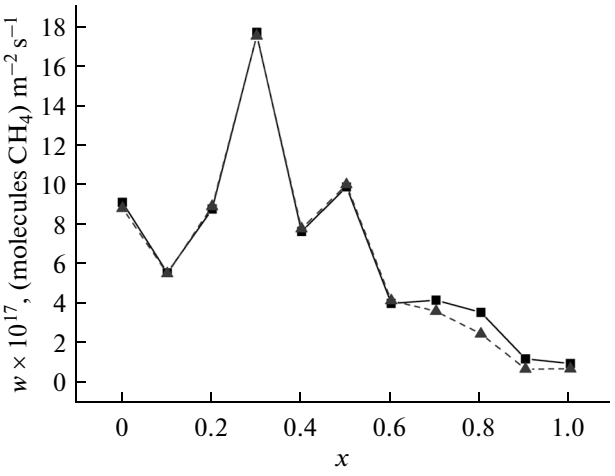

Fig. 7. CO oxidation rate at 350°C as a function of the oxide composition (■) at the early stages of the test and (▲) at the end the test (after lowering the temperature).

For refining the understanding of the effect of methane contained in the reaction medium on the restructuring of the oxides, we measured their activity in CO oxidation in the temperature range from 300 to 500°C. As follows from the results of these experiments, the activity of the oxides at the early stages of testing at 350°C and the activity measured after the cooling of the samples are practically equal (Fig. 7). Therefore, the oxides are more stable in CO oxidation that they are in methane oxidation even at a lower oxygen content of the reaction medium. We also believe that the blocking of the surface by surface carbonates not markedly deactivates the catalysts in methane oxidation. The data obtained in this study indicate that methane exerts a specific effect on the restructuring and vacancy ordering in the substituted perovskites and, accordingly, on the stability of these mixed oxides in methane-containing reaction media.

The increase in the activity of the oxides due to the introduction of calcium up to x = 0.5 and the changes occurring at different reaction temperatures can be described in terms of variations in the proportions of weakly bonded oxygen and vacancies in the oxides and vacancy ordering. It is possible that the iron oxide particles occurring on the surface exert a favorable effect on the catalytic activity and the increased calcium content, which can cause the formation of surface carbonates and, accordingly, block the surface, has an adverse effect on the catalytic activity. However, because the number of iron oxide nanoparticles on the oxide surface increases with an increasing x and in the course of testing, while there is likely no blocking effect of the carbonates, the observed changes in activity are due to the variation of the imperfection of the perovskites.

CONCLUSIONS

The catalytic activity of the substituted lanthanum ferrites synthesized by the Pechini method depends not only on the degree of substitution of calcium for lanthanum but also on the action of the reaction medium. The activity of the homogeneous solid solutions in the $x = 0–0.7$ range passes through a maximum as x is increased. This can be due to variations in the proportions of weakly bonded oxygen and oxygen vacancies in the oxides and in the degree of segregation of these vacancies. The action of the reaction medium and the consequent variation of the imperfection of the oxides cause partial decomposition of the perovskite phase accompanied by the formation of planar defects in the structure of this phase and by the appearance of iron oxide nanoparticles on the surface. This is evidently due to the change in the oxygen content of the material, for similar structural changes were observed by us in the $x > 0.5$ samples upon their heating above 1000°C both in a vacuum and in air. Therefore, the observed decline in the catalytic activity of the oxides in the reaction medium can be caused by the above-described perovskite decomposition processes.

REFERENCES

1. Kharton, V.V., Yaremchenko, A.A., Kovalevsky, A.V., Viskup, A.V., Naumovich, E.N., and Kerko, P.F., *J. Membr. Sci.*, 1999, vol. 163, no. 2, p. 307.
2. Bayraktar, D., Clemens, F., Diethelm, S., Graule, T., van Herle, J., and Holtappels, P., *J. Eur. Ceram. Soc.,* 2007, vol. 27, p. 2455.
3. Hung Ming-Hao, Madhava Rao, M.V., and Tsai Dah-Shyang, *Mater. Chem. Phys.*, 2007, vol. 101, p. 297.
4. Barbero, B.P., Gamboa, J.A., and Cadus, L.E., *Appl. Catal., B*, 2006, vol. 65, nos. 1–2, p. 21.
5. Pinaeva, L.G., Isupova, L.A., Prosvirin, I.P., Sadovskaya, E.M., Ivanov, D.V., and Gerasimov, E.Yu., *Catal. Lett.*, 2013, vol. 143, no. 12, p. 1294.
6. Pérez-Ramírez, J. and Vigeland, B., *Catal. Today*, 2005, vol. 105, p. 436.
7. Ciambelli, P., Cimino, S., Lisi, L., Faticanti, M., Minelli, G., Pettiti, I., and Porta, P., *Appl. Catal., B,* 2001, vol. 33, p. 193.
8. Grenier, J.-C., Pouchard, M., and Hagenmuller, P., *Struct. Bond.*, 1981, vol. 47, p. 1.
9. Isupova, L.A., Yakovleva, I.S., Tsybulya, S.V., Kryukova, G.N., Boldyreva, N.N., Vlasov, A.A., Alikina, G.M., Ivanov, V.P., and Sadykov, V.A., *Kinet. Catal.*, 2000, vol. 41, no. 2, p. 287.
10. Isupova, L.A., Tsybulya, S.V., Kryukova, G.N., Alikina, G.M., Boldyreva, N.N., Vlasov, A.A., Snegurenko, O.I., Ivanov, V.P., Kolomiichuk, V.N., and Sadykov, V.A., *Kinet. Catal.*, 2002, vol. 43, no. 1, p. C.129.
11. Isupova, L.A., Yakovleva, I.S., Tsybulya, S.V., Kryukova, G.N., Boldyreva, N.N., Vlasov, A.A., Rogov, V.A., and Sadykov, V.A., *Chem. Sustainable Dev.*, 2002, vol. 10, p. 27.
12. Nadeev, A.N., Tsybulya, S.V., Gerasimov, E.Yu., Kulikovskaya, N.A., and Isupova, L.A., *J. Struct. Chem.*, 2010, vol. 51, no. 5, p. 891.
13. Nadeev, A.N., *Extended Abstract of Cand. Sci. (Phys.–Math.) Dissertation*, Novosibirsk: Boreskov Inst. of Catalysis, 2008.
14. Price, P.M., Rabenberg, E., Thomsen, D., Misture, S.T., and Butt, D.P., *J. Am. Ceram. Soc.*, 2014, vol. 97, no. 7, p. 2241.
15. Isupova, L.A., Yakovleva, I.S., Rogov, V.A., and Sadykov, V.A., *Kinet. Catal.*, 2004, vol. 45, no. 3, p. 446.
16. Pecchi, G., Jiliberto, M.G., Buljan, A., and Delgado, E.J., *Solid State Ionics*, 2011, vol. 187, p. 27.
17. Nadeev, A.N., Tsybulya, S.V., Belyaev, V.D., Yakovleva, I.S., and Isupova, L.A., *J. Struct. Chem.*, 2008, vol. 49, no. 6, p. 1077.
18. Isupova, L.A., Gerasimov, E.Yu., Zaikovskii, V.I., Tsybulya, S.V., *Kinet. Catal.*, 2011, vol. 52, no. 1, p. 104.
19. Gerasimov, E.Yu., Zaikovskii, V.I., Tsybulya, S.V., and Isupova, L.A., *J. Surf. Invest.*, 2009, vol. 3, no. 5, p. 756.

Translated by D. Zvukov